

Design of a modified three-rail shear test for shear fatigue of composites

I. De Baere, W. Van Paepegem and J. Degrieck

Department of Mechanical Construction and Production, Faculty of Engineering, Ghent University. Sint-Pietersnieuwstraat 41, B-9000 Gent, Belgium.
E-mail: Ives.DeBaere@UGent.be

Abstract

There are various ways of determining the static in-plane shear properties of a fibre reinforced composite. One of them is the standard three-rail shear test, as described in “*ASTM D 4255/D 4255M The standard test method for in-plane shear properties of polymer matrix composite materials by the rail shear method*”. This set-up, however, requires drilling holes through the specimen. In this study, a new design based on friction and geometrical gripping, without the need of drilling holes through the composite specimen is presented. Quasi-static tests have been performed to assess the symmetry of the set-up and the occurrence of buckling. Then, fatigue tests were done to assess the behaviour of the grips under fatigue loading conditions, yielding excellent results; the specimen fails under shear loading conditions in the loaded area. The material used to validate this set-up was a carbon fabric reinforced polyphenylene sulphide.

During fatigue, this material shows an increase in permanent deformation and a decrease in shear stiffness until a certain point in time, after which a drastic increase in deformation and temperature, higher than the softening temperature of the matrix occurs. Furthermore, the maximum value of the shear stress for fatigue with $R = 0$ has a large influence on the fatigue lifetime.

1. Introduction

There are various ways of inducing a state of in-plane shear [1, 2] in a composite. When fatigue loading conditions are required, torsion of thin-walled tubes, sometimes combined with tension or bending in biaxial fatigue [3, 4, 5] is used most of the time. Sometimes, the $[+45^\circ/-45^\circ]_{ns}$ test is used [6], but the rail shear test is rarely considered [7]. The rail shear test, both two-rail and three-rail, as described in the “*ASTM D 4255/D 4255M The standard test method for in-plane shear properties of polymer matrix composite materials by the rail shear method*” has one large disadvantage: it requires drilling holes through the specimen, so that the clamps can be bolted to the specimen. Drilling in composites should be avoided, since it nearly always causes damage to the composite and it may cause stress concentrations around the holes [8]. Furthermore, the preparation of the specimen takes more time. Hussain and Adams tried to remediate these drawbacks with a new design for the two-rail shear test. [8, 9]. This design no longer requires holes in the specimen. However, in these manuscripts, fatigue was not considered.

Lessard et al. [7] did use the three-rail shear setup for fatigue testing, but they did not discuss any fatigue results in their manuscript. Furthermore, they studied a unidirectionally reinforced epoxy.

In this manuscript, a modification for the three-rail shear test is proposed, which no longer requires holes through the specimen, as has been proposed for the two-rail shear test in [8, 9]. Furthermore, this design should allow for fatigue loading conditions, which were not considered by Hussain et al. [8, 9]. The set-up used by Lessard et al. [7] for their fatigue research was the standard three-rail set-up, which requires the holes. The emphasis of their study was the use of notched specimens, in order to avoid preliminary failure of the specimens.

In the next paragraph, the design of the new clamps is discussed. This is followed by the quasi-static and fatigue experiments, done to assess the behaviour of the set-up. Finally, some conclusions are drawn.

2. Design of the set-up

Since the set-up is designed for fatigue loading conditions, some modifications should be made so that the set-up itself does not fail under fatigue loading. Lessard et al. had also made some modifications to the standard three-rail shear set-up [7]. However, for the design presented here, the modifications are far more drastically, since there are no more bolts through the clamp, holding it together. The same principle as in [8, 10] is used, which means that the specimen is gripped by pressing a plate against the specimen. This pressure is applied by bolts which go through only one side of the clamp. However, the force required to press this load transfer plate against the specimen has a similar but opposite reaction force that pushes the two sides of the grip outwards. The latter is clarified in Figure 1 (a), where the different application of the bolts is illustrated.

It is obvious that because of this outward force, the clamps will need to be more massive if they are to withstand the fatigue loading conditions. As a starting point, the grips are designed in one piece, whereas the standard grips are two separate pieces, bolted together. In the grip, a rectangular cavity is milled away for the specimen. Since sharp corners produce unwanted stress concentrations, circular holes are drilled at the ends of this rectangular cavity, to soften the stress concentrations. This results in the grip, of which a cross section is illustrated in Figure 1 (b); some general dimensions are added.

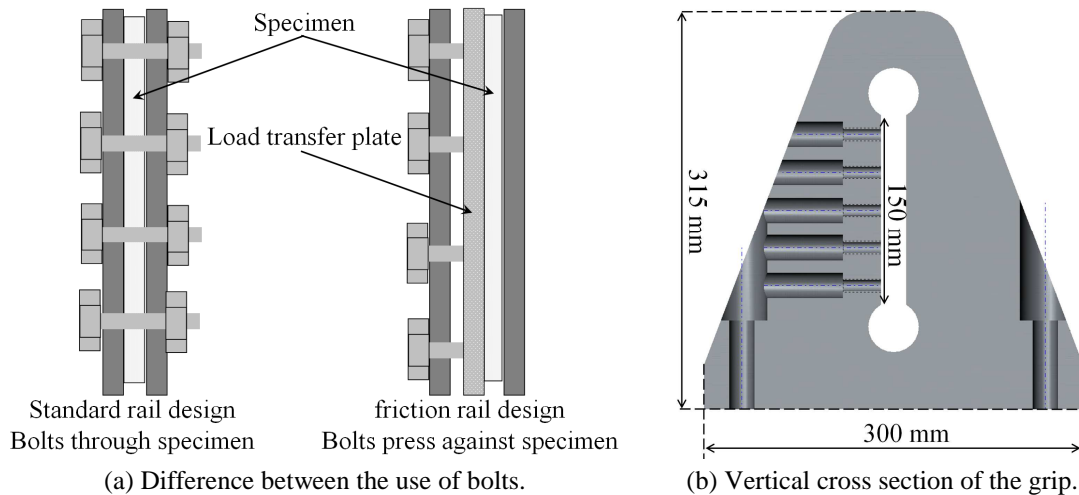


Figure 1 Illustrations of the new design.

The design specifications stated that the grips should be able to withstand the same dynamic load range as the servo-hydraulic tensile machine it is mounted on. This means that the grips should withstand a longitudinal force of 100 kN. Since the gripping is based on friction, a value of the friction coefficient is estimated. The assumption was made (for design purposes) that a friction coefficient of 0.5 should be feasible, with the use of additional rubber films or layers that increase the friction, should the friction between steel and composite be insufficient.

After a few preliminary tests, it became obvious that for some materials, such as the carbon fabric reinforced PPS used for this study, the friction coefficient of 0.5 could not be reached, even if extra layers of high frictional materials were added. In some cases the rubber film was pushed out of the grips, in other cases the film failed under the shear loads. This, however, means that the first gripping design, depicted in Figure 2 (a) and based on pure friction, will not suffice. Therefore, the geometrical gripping was added, which is illustrated in Figure 2 (b). The load transfer plate is now supported by flattened cylinders, so that the load transfer to the grip is not only achieved by friction, but also by these cylinders.

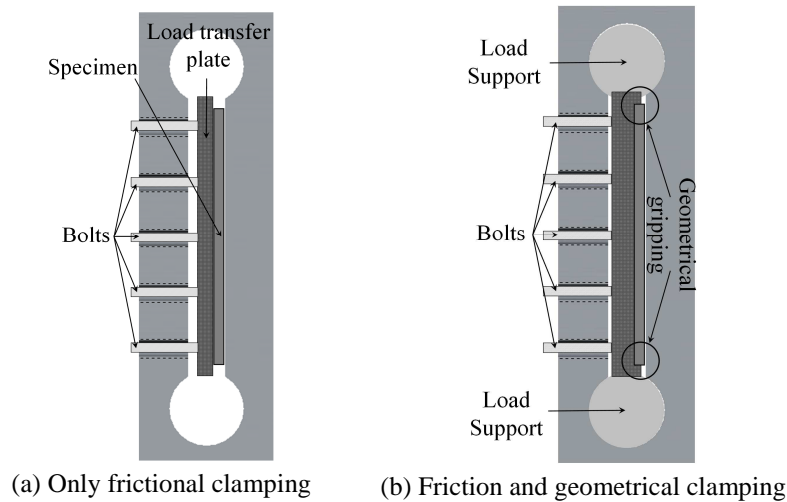


Figure 2 Illustration of the used gripping principles for the proposed design.

For the actual design, the CAD/CAE package ‘Solidworks 2005’ was used. In this package, there is also a finite element module, ‘COSMOS Express’ which was used to determine the stress distribution in the clamp.

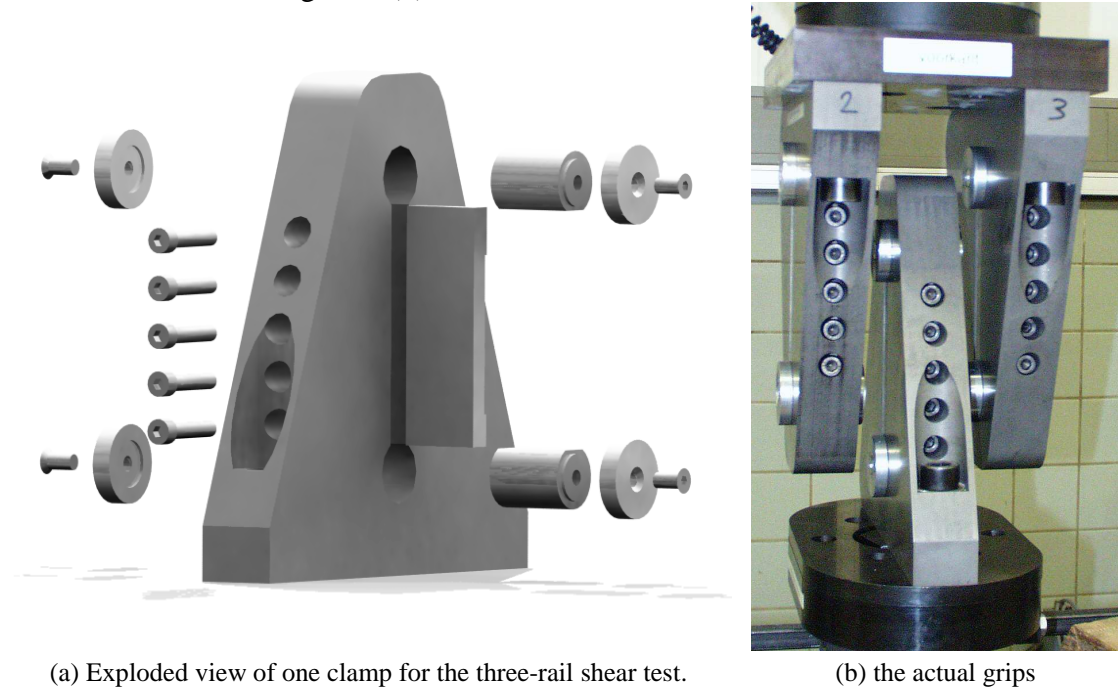
In order to ensure an infinite fatigue life under loading of 100 kN, a safety factor of 3 with respect to the yield stress was taken into account when designing the clamps. Because of the high loads, a high-strength steel was chosen.

In this set-up the central clamp carries the highest load; due to symmetry of the three-rail shear set-up, each of the outer grips carries half the load of the central one. Therefore, the central grip is considered for the simulations. Furthermore, it is assumed that the vertical force of 100 kN is evenly distributed over the two vertical faces, so that each face carries 50 kN. Using a friction coefficient of 0.5, this results in a necessary horizontal load of 100 kN by the load transfer plate on each face. These loading conditions are the worst case scenario for the grips and assume the use of only frictional gripping (Figure 2 (a)). If geometrical gripping is added (Figure 2 (b)), then the horizontal forces will be less, since part of the vertical force is transported via the cylinders to the grips. As such, the vertical load remains the same, the horizontal force will decrease.

In this simulation, the maximum stress level is 154.4MPa, the minimum factor of safety is 3.86 with respect to the estimated yielding stress of 620 MPa. This should ensure infinite fatigue life.

The final design, implementing both frictional and geometrical clamping, is illustrated in Figure 3 (a), as an exploded view. This design was used for all experiments conducted in this manuscript.

Also, two extra plates were designed in order to be able to mount this set-up on a standard servo-hydraulic testing machine. The final set-up, mounted on the tensile machine, is shown in Figure 3 (b).



(a) Exploded view of one clamp for the three-rail shear test.

(b) the actual grips

Figure 3 The final design.

3. Experiments and discussion

3.1. Composite Material

The material used for the experiments was a 5-harness satin-weave carbon fabric-reinforced polyphenylene sulphide (PPS). The carbon PPS plates were hot pressed, one stacking sequence was used for this study, namely $[(0^\circ, 90^\circ)]_{2s}$ where $(0^\circ, 90^\circ)$ represents one layer of fabric. The in-plane elastic properties and the tensile strength properties are listed in Table 1. This material was supplied to us by Ten Cate Advanced Composites (The Netherlands).

Table 1 Elastic and strength properties of the CETEX® material

E_{11} [GPa]	E_{22} [GPa]	ν_{12} [-]	G_{12} [GPa]	X_T [MPa]	ϵ_{11}^{ult} [-]	Y_T [MPa]	ϵ_{22}^{ult} [-]	S_T [MPa]
56.0	57.0	0.033	4.175	736	0.011	754.0	0.013	110.0

The test coupons were sawn with a water-cooled diamond saw. The dimensions of the coupons are shown in Figure 4.

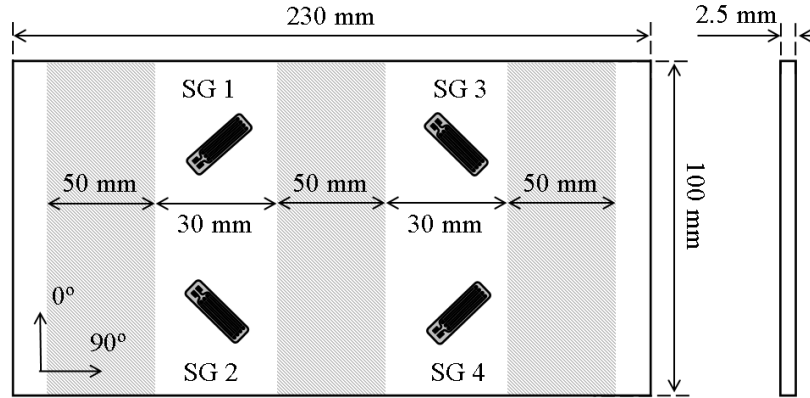


Figure 4 Dimensions of the used specimen, with a $[(0^\circ, 90^\circ)]_{4s}$ stacking sequence. The position of the clamps and strain gauges are also illustrated.

3.2. Equipment

All tensile tests were performed on a servo-hydraulic INSTRON 1342 tensile testing machine with a FastTrack 8800 digital controller and a load cell with a dynamic range of ± 100 kN.

For the registration of the test data, a combination of a National Instruments DAQpad 6052E for FireWire, IEEE 1394 and the SCB-68 pin shielded connector were used. The load and displacement, given by the FastTrack controller, as well as the extra signals from the strain gauges were sampled on the same time basis.

3.3. Quasi-static experiments

The desired stress state for this set-up is to have pure and equal shear load for both of the loaded zones. However, due to misalignment of the clamps, the zones on the left and the right of the central clamp may not experience the same load. Furthermore, buckling or bending of the specimen may occur, which means that the front and the back of one loaded zone (left or right) may have a different stress state. Hence, a few quasi-static tests were done to assess the occurrence of buckling and whether the set-up induces a symmetrical load. Both types of tests were done in a displacement controlled manner with a displacement speed of 1 mm/min; the signals were sampled at 20 Hz. Furthermore, quasi-static cyclic loading (hysteresis) was applied, starting with a shear stress of 10 MPa and increasing with 10 MPa each cycle until the strain gauges saturated or de-bonded. By performing these cyclic loadings, possible problems regarding symmetry or buckling will be more easily detected than in a quasi-static test with monotonic loading until saturation or de-bonding of the gauges, because differences in the strains will probably increase with each successive loading, due to permanent deformation of the specimen.

To verify the symmetry, four strain gauges were placed on the same side of the specimen, but distributed over the two loaded zones, as illustrated on Figure 4. The time evolution of the different strain gauges for such a test is given in Figure 5 (a). If the set-up is symmetrical, then strain gauge 1 and 3 and strain gauge 2 and 4 respectively should give the same strain. It can clearly be seen that the signals coincide almost perfectly, meaning symmetry is achieved. The de-bonding or failing of the strain gauges can also be seen: after about 350 seconds, strain gauge 3 de-bonded; after 450 s, gauge 1

failed and after 500 s, gauge 2 failed. Gauge 4 failed soon after gauge 2. As a result; the corresponding curves no longer coincide from that point on.

To assess whether buckling occurs, the four strain gauges are placed on the same loaded zone, but on front and rear surfaces. Strain gauges 1 and 2 are placed as depicted in Figure 4 and strain gauges 3 and 4 are placed on the same position on the opposite side of the specimen in such a way that the strains from strain gauge 1 and 2 should correspond with the signals from strain gauges 3 and 4 respectively. The result from such a test is depicted in Figure 5 (b). Again, the signals coincide almost perfectly. Similar to the previous test, the curves are only shown until the strain gauges de-bonded. This happened at 470 s for gauge 3 and at 510 s for gauge 4. The other gauges failed soon after 600 s.

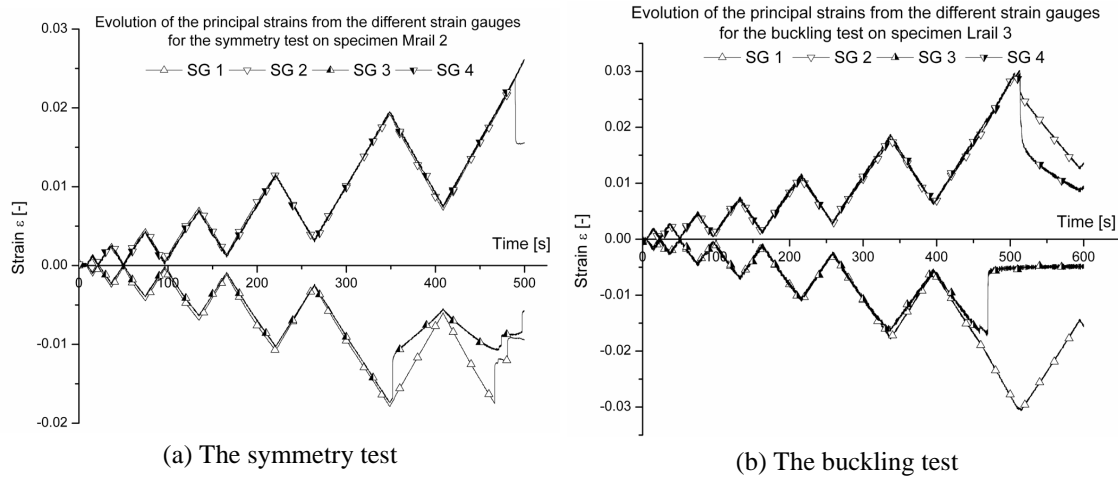


Figure 5 Evolution of the strain as a function of time for all four strain gauges in symmetry and buckling test.

Similar experiments have been conducted, all with corresponding results. As such, it may be concluded that the stress state induced by the clamps is symmetrical and that no buckling or bending of the specimen occurs. As a result, there is no longer need for four strain gauges, two strain gauges, mounted on the same surface of one loaded zone under $+45^\circ$ and -45° suffice for the measurement, for instance gauges 1 and 2 or 3 and 4 in Figure 4.

For both measurements mentioned above, the temperature was also monitored, using a thermocouple. Because of the shear loads, a temperature increase is expected. However, no significant increase in temperature was detected.

To verify the evolution of the shear stress as a function of the shear strain, three quasi-static tests, instrumented with strain gauges, were done. For comparison, two quasi-static tensile tests, as described by the “*ASTM D 3518 - 76 Standard practice for in-plane shear stress-strain response of unidirectional reinforced plastics*” were done on a $[(+45^\circ, -45^\circ)]_{4s}$ specimen. The results are shown in Figure 6, the curves are depicted until the strain gauges either de-bonded or saturated. It must be noted that these curves correspond well, even for the uni-axial tests on the $[45^\circ, -45^\circ]_{4s}$ specimens. The shear stiffness is found by taking the tangent modulus in the origin. It must be noted that these values show good correspondence with the value given in Table 1. Since four strain gauges were mounted on the rail shear specimens, two shear stress-strain curves could be calculated. However, in Figure 6 only the curve from the strain gauges which lasted the longest (de-bonding or saturation) is shown.

As a result, the maximum shear strain depicted on the graph is not the failure strain. For the rail shear specimens, the tests were stopped after the gauges de-bonded, to assess the permanent deformation after unloading and to keep the specimen intact for further non-destructive testing. The $[(+45^\circ, -45^\circ)]_{4s}$ specimens, however, were loaded until failure occurred at 105 MPa, which is in good correspondence with the value in Table 1.

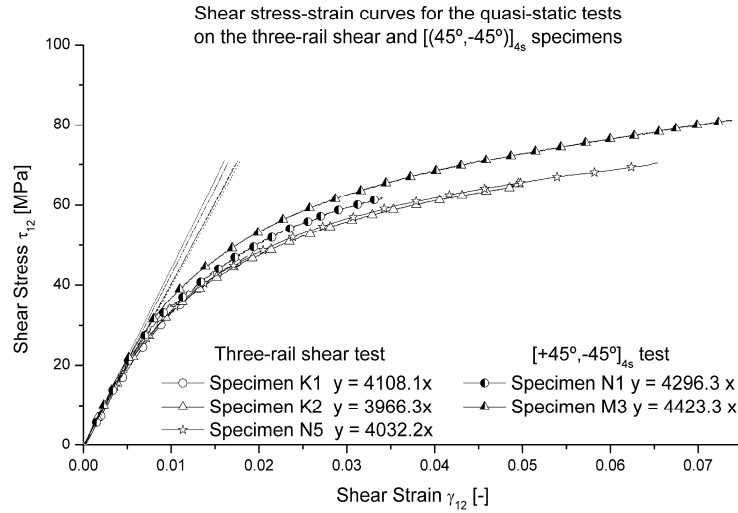


Figure 6 Shear stress – strain evolution for the quasi-static rail shear tests. A uni-axial test according to the ASTM D 3518 – 76 is added for comparison.

Because of the combined frictional and geometrical clamping of the design, this set-up has another interesting advantage. Given the definition of the shear strain γ (Figure 7), it can be calculated as:

$$\tan \gamma = \frac{D}{W} \quad (1)$$

If small displacements are assumed, the shear strain will be small and can be calculated as:

$$\tan \gamma \approx \gamma \approx \frac{D}{W} \quad (2)$$

This means that there should be a linear correlation between the shear strain γ and the imposed displacement from the central rail D , given by ($W = 30$ mm, see Figure 4)

$$\gamma = \frac{1}{30} D = 0.033D \quad (3)$$

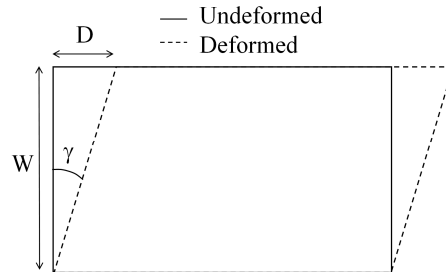


Figure 7 Definition of the shear strain γ .

During the experiments it was noted that there is a correlation between the imposed displacement and the resulting shear strain in the specimen, but it is rather parabolic than linear.

This is illustrated in Figure 8; the different experiments are given an offset along the x-axis for a clear image. It can be noted that for both the hysteresis tests, the curves are very reproducible.

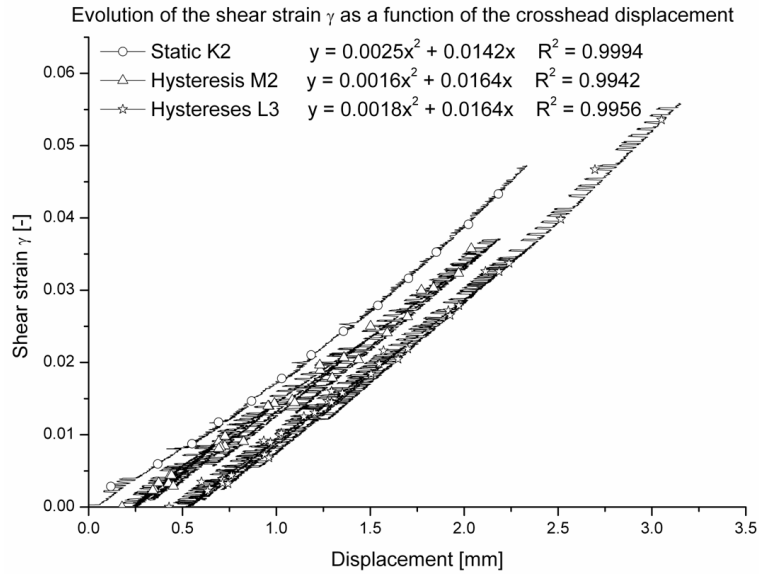


Figure 8 Illustration of the correlation between shear strain and displacement.

The reason for the difference between the experimental and theoretical correlation can be explained as follows. Theoretically, a displacement of 2 mm on the side edge is exactly 2 mm, whereas a displacement of 2 mm of the plunger will be less than 2 mm displacement of the side edge of the loaded zone, because of the following reasons: (i) the height of the specimen is not exactly equal to the height of the geometrical gripping, since then, mounting the specimen would be practically impossible. As a result, some slippage may occur. (ii) The load transfer plates do not fit exactly in the space provided, the height is a little less since otherwise, the plates could not be mounted. Again, some slippage may occur. (iii) The mounting mechanism on the tensile machine, as well as the tensile machine deforms under the occurring loads. Hence, the displacement of the side of the specimen will always be a little smaller than the imposed displacement by the plunger. This is the same reason why the calculated strain from the displacement in a uni-axial tensile test differs from the strain, measured with extensometer or strain gauges.

It is expected that a similar phenomenon is present when using the standard three-rail shear test set-up. However, nothing on this matter is documented by Lessard et al. [7].

3.4. Fatigue experiments

Since the design has proven to provide reliable and reproducible results, fatigue experiments are considered. Because of the large displacements, these tests were done without strain gauges, since they would de-bond after a few dozens of cycles. However, an estimation of the occurring shear strain levels can still be made, because of reproducible correlation between shear strain and displacement for the hysteresis tests and as result, the evolution of the shear strain will be similar to that of the displacement. Besides load and displacement, the temperature was also monitored during the experiment. Every five minutes five loading cycles were recorded and from these signals, the maximum, minimum and average values were calculated.

A first load controlled fatigue test was done with the shear stress between 0 and 40 MPa ($R = 0$) at a frequency of 2 Hz. The maximum shear stress is about 36% of the shear strength. The results are given in Figure 9 (a). It should be noted that there is a gradual increase of both the mean value of the displacement and its amplitude. Given the fact that it was a load controlled test, this means that permanent deformation and shear stiffness reduction occurs. At a certain point in time, around 1,150,000 cycles, the slope of the displacement curves starts increasing and little later, there is a significant rise in temperature. The softening temperature of the polyphenylene matrix is 90 °C but even before this temperature is reached, very large displacements occur. This can probably be explained by the fact that the temperature is registered at the surface of the specimen and the temperature inside the specimen will be higher, since the surface is cooled by the surrounding airflow. Because of the very large displacements and large increase in temperature, the test was stopped before failure at 1,396,165 cycles. Again, because of the linearity between shear strain and displacement, the same conclusions as for the displacement could be made for shear strain.

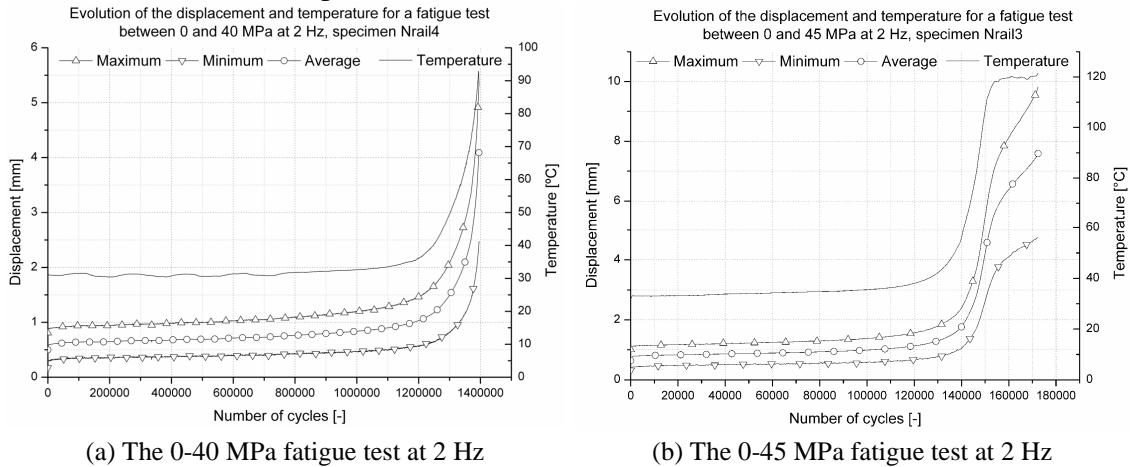


Figure 9 Maximum, minimum and mean value of the displacement as a function of the number of cycles.

A second load controlled test was done, but at a slightly higher maximum shear stress. This test was done at 2 Hz and between 0 and 45 MPa ($R = 0$); the latter is about 40% of the shear strength;. The corresponding results are shown in Figure 9 (b). The same remarks concerning the displacement and temperature as for the previous test can be made, but it should be noted that these effects start a lot earlier. The increase in temperature and displacement occurs after only 130,000 cycles, which is a lot less than the 1,150,000 cycles from the previous test, and this only from an increase in maximum load of 5 MPa. This specimen failed overnight, so it was not stopped before failure and as a result, a temperature of 120 °C was reached at the surface of the specimen. The resulting softening of the matrix of course causes the large deformations.

Finally, it should be remarked that for most specimens, although fracture initiated near the clamp ends on the side of the specimen, final failure occurred in the shear loaded zone in the middle of section.

4. Conclusions

A modified design of the standard three-rail shear set-up, as described in “ASTM D 4255/D 4255M The standard test method for in-plane shear properties of polymer matrix composite materials by the rail shear method” has been presented.

This new design uses friction and geometrical gripping, without the need of drilling holes through the composite specimen. Quasi-static tests to assess the symmetry of the set-up and the occurrence of buckling have been performed with very good results; both sides of the specimen are loaded symmetrically and no buckling occurs. The shear stiffness, derived from the static tests is in good correspondence with the stiffness determined by the dynamic modulus identification method and the $[(45^\circ, -45^\circ)]_{4s}$ test. Finally, fatigue tests have been performed to assess the behaviour of the grips under fatigue loading conditions, with excellent results; the specimen fails under shear loading conditions in the loaded area. The material itself has an increase in permanent deformation and a decrease in shear stiffness until a certain point in time, after which a drastic increase in deformation and temperature occurs. The latter exceeds the softening temperature of the polyphenylene matrix. The maximum value of the shear stress amplitude for fatigue with $R = 0$ has a large influence on the fatigue lifetime. Future work will concentrate using this new set-up for modelling the shear behaviour of the carbon fabric reinforced polyphenylene sulphide, both under quasi-static and fatigue loading conditions.

Acknowledgements

The authors are highly indebted to the university research fund BOF (Bijzonder Onderzoeksfonds UGent) for sponsoring this research and to Ten Cate Advanced Composites for supplying the material.

References

- [1] Tarnopol'skii YM, Arnautov AK, Kulakov VL, Methods of determination of shear properties of textile composites. COMPOSITES PART A-APPLIED SCIENCE AND MANUFACTURING 30 (7): 879-885 1999.
- [2] Whitney, J.M., Daniel, I.M. and Pipes, R.B. (1984). Experimental mechanics of fiber reinforced composite materials. Chapter 4: Composite characterization. Connecticut, The Society for Experimental Mechanics, pp. 160-202.
- [3] El-Assal, Ahmed M., Khashaba, U. A., Fatigue analysis of unidirectional GFRP composites under combined bending and torsional loads. COMPOSITE STRUCTURES 79 (4): 599-605 AUG 2007
- [4] Qi, Dongtao, Cheng, Guangxu, Fatigue behavior of filament-wound glass fiber reinforced epoxy composite tension/torsion biaxial tubes under loading. POLYMER COMPOSITES 28 (1): 116-123 FEB 2007.
- [5] Kawakami H, Fujii TJ, Morita Y, Fatigue degradation and life prediction of glass fabric polymer composite under tension torsion biaxial loadings. JOURNAL OF REINFORCED PLASTICS AND COMPOSITES 15 (2): 183-195 FEB 1996
- [6] Shalom S, Harel H, Marom G, Fatigue behaviour of flat filament-wound polyethylene composites. COMPOSITES SCIENCE AND TECHNOLOGY 57 (9-10): 1423-1427 1997
- [7] Lessard, L.B., Eilers O.P., Shokrieh M.M., Testing of in plane shear properties under fatigue loading. JOURNAL OF REINFORCED PLASTICS AND COMPOSITES 14 (9): 965-987 SEP 1995
- [8] Hussain AK, Adams DF , Experimental evaluation of the Wyoming-modified two-rail shear test method for composite materials. EXPERIMENTAL MECHANICS 44 (4): 354-364 AUG 2004.
- [9] Hussain AK, Adams DF, Analytical evaluation of the two-rail shear test method for composite materials. COMPOSITES SCIENCE AND TECHNOLOGY 64 (2): 221-238 FEB 2004
- [10] Hussain AK, Adams DF, The Wyoming-modified two-rail shear test fixture for composite materials. JOURNAL OF COMPOSITES TECHNOLOGY & RESEARCH 21 (4): 215-223 OCT 1999.